THE JOURNAL OF PHYSICAL CHEMISTRY Letters

Letter

pubs.acs.org/JPCL

Differential Impact of the Monovalent Ions Li^+, Na^+, K^+, and Rb^+ on DNA Conformational Properties

Alexey Savelyev and Alexander D. MacKerell, Jr.*

Department of Pharmaceutical Sciences, School of Pharmacy, University of Maryland, 20 Penn Street, Room 629, Baltimore, Maryland 21201, United States

Supporting Information

ABSTRACT: The present report demonstrates that the conformational properties of DNA in solution are sensitive to the type of monovalent ion. Results are based on the ability of a polarizable force field using the classical Drude oscillator to reproduce experimental solution X-ray scattering data more accurately than two nonpolarizable DNA models, AMBER Parmbsc0 and CHARMM36. The polarizable model is then used to calculate scattering profiles of DNA in the presence of four different monovalent salts, LiCl, NaCl, KCl, and RbCl, showing the conformational properties of DNA to vary as a function of ion type, with that effect being sequence-dependent. The primary conformational mode associated with the variations is contraction of the DNA minor groove width with decreasing cation size. These results indicate that the Drude polarizable model provides a more realistic representation of ion−DNA interactions than additive models that may lead to a new level of understanding of the physical mechanisms driving salt-mediated biological processes involving nucleic acids.

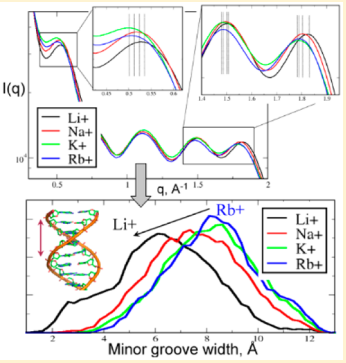

Conformational characterization of DNA in solution still remains a challenge, including understanding the impact of ion type on structural and dynamical properties. While X-ray crystallography and solution NMR are the primary tools used to experimentally study DNA structure,[1] there are limitations on the their ability to fully represent DNA conformational properties in solution. In the case of X-ray crystallography, the DNA molecule is subject to crystal packing forces, which may affect its local and global geometric characteristics.[2,3] Solution NMR is often limited in its ability to model the overall DNA conformation, and structure refinement depends on the underlying mathematical framework,[4] which may lead to conflicting structural models. Alternatively, a solution technique, X-ray diffraction "fingerprinting", is capable of differentiating between the conflicting crystallographic and NMR DNA structures[5] and can serve as a robust tool for the evaluation of the quality of computational models used to investigate DNA.[6] This technique differs from X-ray crystallography in that the solution scattering pattern represents a concise but faithful representation of the full range of DNA dynamics in solution in terms of a limited number of dominant macromolecular conformational modes (1D "fingerprint"), with finer details being averaged over, a concept very similar to the way the complex multidimensional landscape of a protein in its native state is reduced to several essential energetic basins of low dimensionality.[7] Therefore, the information content of solution scattering data allows for unique insights into DNA conformational properties in solution as well as being of utility for the validation of empirical force fields.

In the current study, the recently developed polarizable force field for DNA based on the classical Drude oscillator model[8,9] is shown to quantitatively reproduce the experimentally measured solution-state X-ray diffraction profiles of a number of B form DNA sequences.[5] This contrasts results from two commonly used computational atomistic DNA force fields, the state-of-the-art additive CHARMM36 (C36)[10] and AMBER Parmbsc0[11] models, with respect to their ability to capture the essential DNA conformational properties in solution. In addition, simulated spectra of DNA solvated in aqueous solutions containing different monovalent salts, LiCl, NaCl, KCl, and RbCl, address an important question in the field of DNA biophysics: are differential effects of ion type present and how strong are those effects on DNA conformational properties? Because DNA under physiological conditions is exposed to a mixture of several (mono- and divalent) ionic species, it is important to understand the impact of those ions individually on DNA structure. Studies to date on this topic are limited. Experiments on the compaction of T4 DNA have shown differential effects of monovalent ions;[12] however, no data are available on the differential impact of ion type on small DNA molecules, a necessary step required to understand ion effects in more complex systems. As we report, the type of monovalent ion does impact the solution conformational properties of DNA as observed in MD simulations using a force field that includes the explicit treatment of electronic polarizability using the classical Drude oscillator model. This represents an experimentally untested prediction of the model that is anticipated to set the foundation for further experimental and computational studies of the impact of ion type on DNA conformational properties, information that will help us to

Received: November 20, 2014
Accepted: December 19, 2014
Published: December 22, 2014

DOI: 10.1021/jz5024543
J. Phys. Chem. Lett. 2015, 6, 212−216

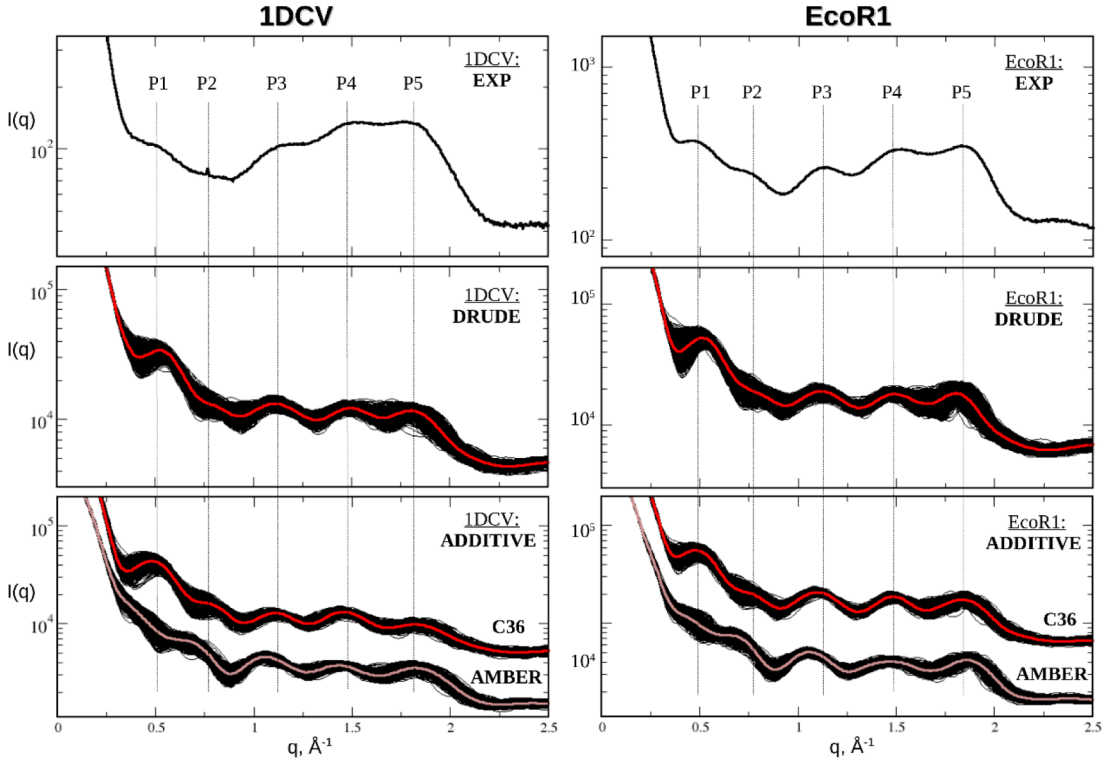

Figure 1. Solution scattering profiles for the 1DCV and *Eco*RI systems from the experiments (upper row) and computed from MD simulations utilizing Drude polarizable (middle row) and additive CHARMM36 and AMBER Parmbsc0 (lower row) DNA models solvated in ∼100 mM NaCl ionic buffer. Positions of the experimental peaks are projected onto the computational results. Intensities for the additive AMBER and C36 systems are shifted with respect to each other to facilitate their comparison.

better understand issues such as competitive ionic binding to DNA,[13] salt-driven nucleic acid array condensation,[14] and other salt-mediated biological processes involving DNA.

Because of the dynamics of DNA in solution, a typical solution X-ray diffraction pattern represents a collection of diffuse peaks, whose number, breadth of dispersion, and positions are unique for a particular sequence. The orientational averaging allows the intensity of molecular scattering to be represented by a mathematically tractable formula in which all vectorial quantities (wave-vector and radius-vector) are reduced to their scalar values. (See the Supporting Information, SI, for details.) Intensities at small wave numbers contain information on the overall shape and size of DNA in solution, while those at higher wave numbers provide structural details arising from spatially resolved atomic correlations within the macromolecule. For example, on the basis of decomposition of the molecular DNA structure into the nucleic acid bases and sugar−phosphate backbones, it was demonstrated that the last major peak of the spectra (at $q \approx 1.7$ to 2.1 Å^{-1}) corresponds primarily to the geometry of the base pair stacking, while the spectral pattern in the range of $q \approx 0.2$ to 1.7 Å^{-1} reflects the combined contribution from the sugar and phosphate moieties.[5,6]

Presented in Figure 1 are solution scattering profiles for two self-complementary B form DNA sequences, d(CGCGAATTCGCG)2 and d(CGCTAGCG)2 from experiments[5] and MD simulations utilizing the Drude polarizable and additive C36 and AMBER Parmbsc0 force fields. In what follows, we refer to these molecules as *Eco*RI and 1DCV, respectively. The first structure is also known as the Drew−Dickerson dodecamer, one of the most studied DNA sequences to date.[15]

The second, 1DCV, is a 10-base-pair crystal structure[16] that contains one extra base pair at each termini as compared with the sequence studied in solution scattering experiments.[5] To be consistent with those experiments, only the internal eight base pairs of 1DCV were used in the calculation of the spectra. (See the SI for details on MD simulation protocols.) As seen in Figure 1, the Drude polarizable and C36 additive models generate scattering spectra consistent with experiment for both systems studied, with the number of peaks (P1−P5) and their approximate positions corresponding to those observed experimentally. In contrast, the AMBER profiles lack a discernible first peak for both systems, with the position of the rest of peaks deviating from experimental positions. For a more quantitative comparison, the peak positions were determined and rms deviations computed between the experimental and simulation results (Table 1). The best agreement with experiment occurs with the Drude model, followed by the additive C36 model, with the AMBER results deviating the most. Discrepancies between experiment and MD simulations of *Eco*RI were observed previously in a previous AMBER DNA force field,[6] where an analogous mismatch in the peak positions and the failure to generate the first major scattering peak (P1) occurred. The scattering results correlate with the magnitudes of structural rms differences (rmsd) of the 1DCV and *Eco*RI molecules with respect to ideal B form DNA (see Figure S1A, SI). In particular, the largest rmsd's are generated by the AMBER force field, with lesser values obtained for the C36 and Drude models. Additionally, a visual comparison of the structures from the Drude, C36, and AMBER simulations reveals significant differences in the overall shape of the macromolecule (see Figure S1B, SI), consistent with the observed differences in the scattering profiles.

DOI: 10.1021/jz5024543
J. Phys. Chem. Lett. 2015, 6, 212−216

Table 1. Peak Positions Inferred from Experimental and Computational Solution Scattering Profiles

		MD[a]		
peak	EXP	C36	AMBER	DRUDE
	*Eco*RI, 12 base pairs			
P1	0.456	0.442		0.507
P2	0.750[b]	0.800[b]	0.640[b]	0.785[b]
P3	1.127	1.101	1.055	1.117
P4	1.513	1.478	1.472	1.490
P5	1.834	1.829	1.861	1.803
rmsd (P2 − P5)		0.033	0.084	0.018
rmsd_all		0.030		0.027
	1DCV, 10 base pairs[c]			
P1	0.510	0.480		0.520
P2	0.755[d]	0.800[d]	0.700[d]	0.820[d]
P3	1.180	1.100	1.050	1.110
P4	1.525	1.455	1.435	1.495
P5	1.790	1.825	1.830	1.800
rmsd (P2 − P5)		0.060	0.086	0.050
rmsd_all		0.055		0.045

[a]Peak positions were determined from zero crossing points in the first derivative; values are in Å^{-1}. [b]Approximate positions of the plateau at P2. [c]Only internal eight base pairs were considered to be consistent with the experimentally studied sequence. [d]Approximate positions of the spike at P2.

The above results were obtained for DNA molecules solvated in an ∼100 mM NaCl aqueous buffer. However, the experimental conditions contained an additional ∼50 mM Tris·HCl.[5] Therefore, we repeated the additive C36 MD simulations of *Eco*RI and 1DCV molecules immersed in a ∼100 mM NaCl with ∼50 mM Tris·HCl aqueous buffer and recomputed the DNA scattering profiles to find out if the altered conditions affect the results. As shown in the Figure S2 of SI, the presence of Tris·HCl did not lead to any noticeable differences in the spectra.

A more intriguing picture emerges when ion type is altered from Na^+ to other monovalent ionic species, including Li^+, K^+, and Rb^+. Figure 2 shows scattering profiles for 1DCV and *Eco*RI simulated in LiCl, NaCl, KCl, and RbCl aqueous buffers using the Drude polarizable and C36 additive force fields. The striking observation is that the Drude polarizable model predicts the different ions to alter the conformational properties of the DNA. Such variation is not present with the additive C36 force field, a result that was also obtained with AMBER for 1DCV (not shown). Among all spectral peaks, the biggest variation is observed for the first (P1) and the two last major peaks (P4, P5), indicating that both local and global DNA geometric parameters are affected. Structural analysis identified significant variation in the minor groove width as a function of ion type (see Figure 3 and Table S1, SI). In addition, some helicoidal parameters demonstrated variations (see Figure S3, SI). Interestingly, no significant variability of the major groove width with ion type was observed (see Figure S4, SI).

Notably, the extent of the variations is much larger for 1DCV versus EcoR1, which may indicate that the observed effect is sequence-specific. To address this possibility, we performed a similar analysis on an additional sequence, d(CGCATGCTA-CGC), a structure recently resolved by solution NMR (PDB: 2L8Q).[17] This sequence is the same length as *Eco*RI but does not possess an AATT-tract. The solution spectra for all four ionic buffers and the minor groove width distributions are shown in the Figure S5 in the SI and Figures 3E,F, respectively. Additionally, distributions for selected helicoidal parameters affected the most by the changes in ionic environment are

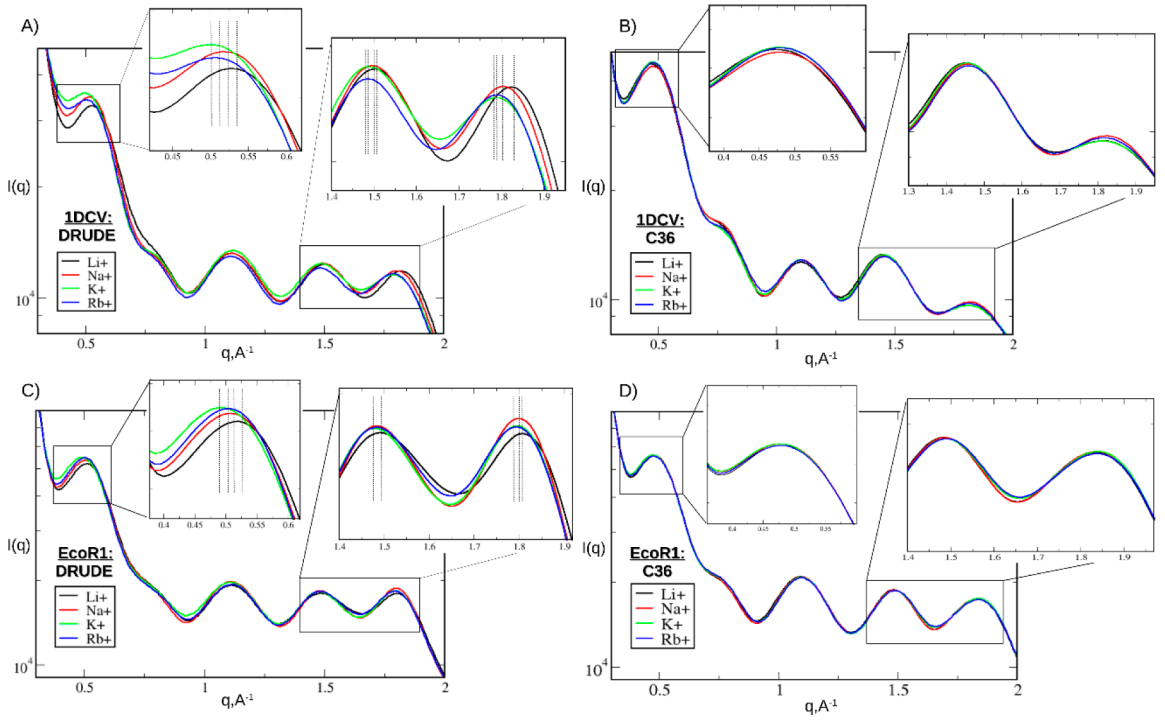

Figure 2. Solution scattering profiles computed from the Drude polarizable (A,C) and CHARMM36 additive (B,D) MD simulations of the 1DCV and *Eco*RI DNA sequences solvated in LiCl, NaCl, KCl, and RbCl containing aqueous buffers. For the Drude model demonstrating spectral variability with the ion type, the approximate positions of the first and two last peaks are schematically shown.

DOI: 10.1021/jz5024543
J. Phys. Chem. Lett. 2015, 6, 212−216

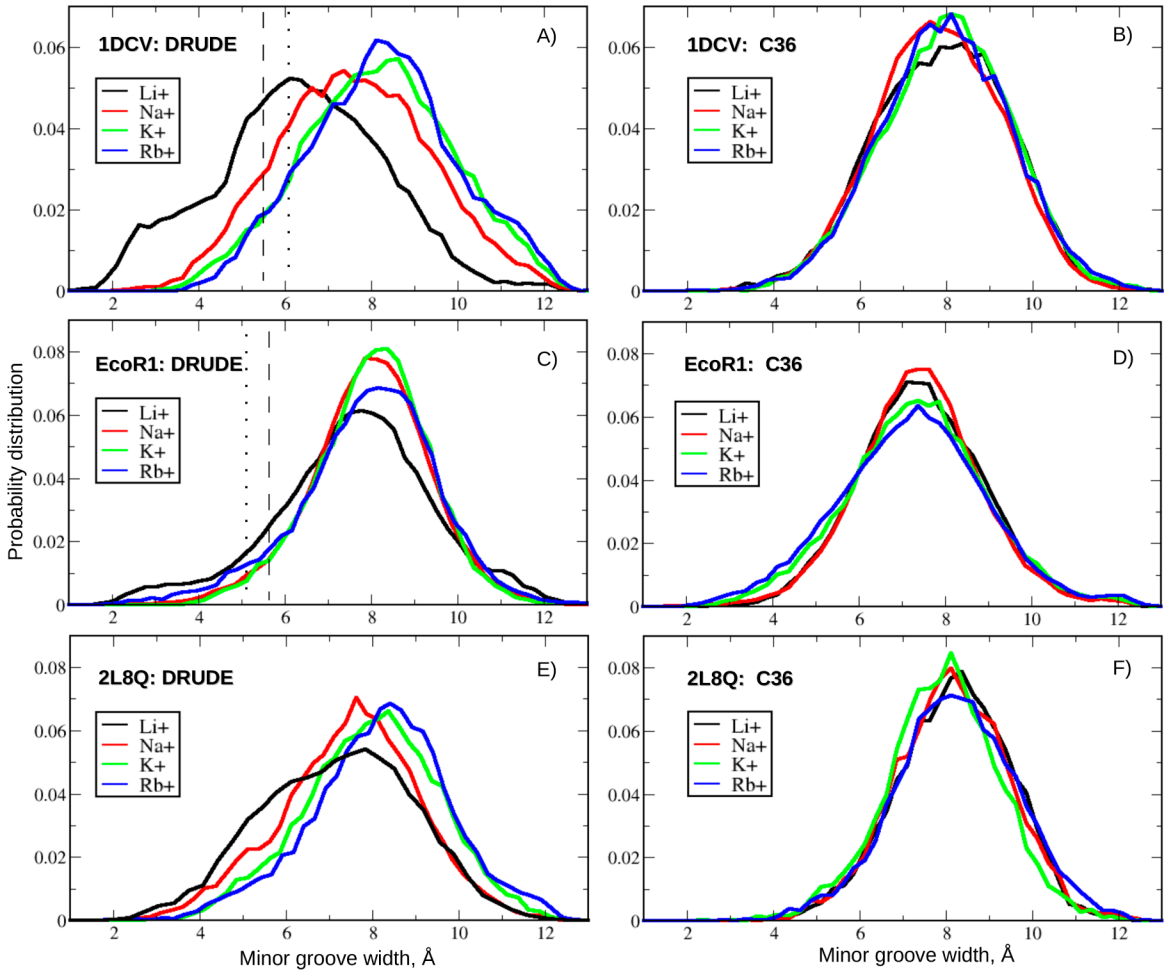

Figure 3. Probability distributions for the minor groove width computed from the Drude polarizable and additive CHARMM36 MD simulations of the 1DCV, *Eco*RI, and 2L8Q DNA systems solvated in various monovalent ionic buffers. For comparison, estimates of the minor groove width inferred from selected NMR (PDB for 1DCV: 1G80; PDB for *Eco*RI: 1DUF) and crystallographic (PDB for 1DCV: 250D; PDB for *Eco*RI: 1BNA) structures are shown in panels A and C as dashed and dotted lines, respectively.

shown in the Figure S3 in the SI. 2L8Q demonstrates an intermediate propensity for its conformation to change due to the different ions relative to *Eco*RI and 1DCV, with the trend remaining the same for the changes in the spectral patterns, the minor groove width, and selected helicoidal parameters. The general feature observed in all systems is that the DNA spectral profiles are uniformly shifted to higher values of the scattering vector as a function of ion size with $Rb^+ < K^+ < Na^+ < Li^+$. The minor groove width is the structural feature correlating the most with the spectral changes, although variations in translational and rotational helicoidal parameters, such as tilt, roll, twist, propeller twist, and shift, also contribute to the overall picture. These results indicate a decrease in the minor groove width for the above series. Additional analyses of the structural changes along with molecular details of specific interactions involving the ions are ongoing and will be reported in a future study.

The present findings as well as the results based on prior computational studies utilizing Drude polarizable DNA model[9,18] indicate that inclusion of polarization effects indeed provides more realistic representation of the many-body effects in the DNA polyion and the interactions of DNA with its ionic environment. The differences in conformational properties as a function of ion type predicted by the model are notable, with those effects being sequence-dependent. To date, no experimental scattering studies of the role of ion type on DNA conformation have been performed. Thus, these results prompt for additional solution-scattering experiments involving more DNA sequences and ionic buffers. In this light, Drude polarizable MD simulations may offer the potential to yield new insights into salt-mediated biological processes involving DNA, such as protein−DNA recognition and chromatin folding.

■ ASSOCIATED CONTENT

Supporting Information

MD simulation protocols, implementation of the routing calculating solution scattering profiles from MD simulations, description of the DNA structural analysis, and supplementary figures and tables. This material is available free of charge via the Internet at http://pubs.acs.org.

■ AUTHOR INFORMATION

Corresponding Author

*E-mail: alex@outerbanks.umaryland.edu. Phone: (410) 706-7442. Fax: (410) 706-5017.

Notes

The authors declare no competing financial interest.

DOI: 10.1021/jz5024543
J. Phys. Chem. Lett. 2015, 6, 212−216

■ ACKNOWLEDGMENTS

We acknowledge the NIH (GM051501) for financial support and the University of Maryland Computer-Aided Drug Design Center and the XSEDE resources for their generous allocations of computer time. We thank Dr. Xiaobing Zuo for providing experimental solution scattering data used in this study and Drs. Nathan Baker, Alexey Onufriev, and Marc Taraban for helpful discussions.

■ REFERENCES

(1) Berman, H. M.; Olson, W. K.; Beveridge, D. L.; Westbrook, J.; Gelbin, A.; Demeny, T.; Hsieh, S.-H.; Srinivasan, A. R.; Schneider, B. The Nucleic Acid Database: A Comprehensive Relational Database of Three-Dimensional Structures of Nucleic Acids. *Biophys. J.* **1992**, *63*, 751−759.

(2) Abrescia, N. G. A.; Thompson, A.; Huynh-Dinh, T.; Subirana, J. A. Crystal Structure of an Antiparallel DNA Fragment with Hoogsteen Base Pairing. *Proc. Natl. Acad. Sci. U.S.A.* **2002**, *99*, 2806−2811.

(3) Abrescia, N. G. A.; Gonzalez, C.; Gouyette, C.; Subirana, J. A. X-ray and NMR Studies of the DNA Oligomer d(ATATAT): Hoogsteen Base Pairing in Duplex DNA. *Biochemistry* **2004**, *43*, 4092−4100.

(4) Kuszewski, J.; Schwieters, C.; Clore, G. M. Improving the Accuracy of NMR Structures of DNA by Means of a Database Potential of Mean Force Describing Base-Base Positional Interactions. *J. Am. Chem. Soc.* **2001**, *123*, 3903−3918.

(5) Zuo, X. B.; Tiede, D. M. Resolving Conflicting Crystallographic and NMR Models for Solution-State DNA with Solution X-ray Diffraction. *J. Am. Chem. Soc.* **2005**, *127*, 16−7.

(6) Zuo, X. B.; Cui, G. L.; Merz, K. M.; Zhang, L. G.; Lewis, F. D.; Tiede, D. M. X-ray Diffraction "Fingerprinting" of DNA Structure in Solution for Quantitative Evaluation of Molecular Dynamics Simulation. *Proc. Natl. Acad. Sci. U.S.A.* **2006**, *103*, 3534−3539.

(7) Materese, C. K.; Goldmon, C. C.; Papoian, G. A. Hierarchical Organization of Eglin C Native State Dynamics is Shaped by Competing Direct and Water-Mediated Interactions. *Proc. Natl. Acad. Sci. U.S.A.* **2008**, *105*, 10659−10664.

(8) Savelyev, A.; MacKerell, A. D., Jr. All- Atom Polarizable Force Field for DNA Based on the Classical Drude Oscillator Model. *J. Comput. Chem.* **2014**, *35*, 1219−1239.

(9) Savelyev, A.; MacKerell, A. D., Jr. Balancing the Interactions of Ions, Water, and DNA in the Drude Polarizable Force Field. *J. Phys. Chem. B* **2014**, *118*, 6742−6757.

(10) Hart, K.; Foloppe, N.; Baker, C. M.; Denning, E. J.; Nilsson, L.; MacKerell, A. D., Jr. Optimization of the CHARMM Additive Force Field for DNA: Improved Treatment of the BI/BII Conformational Equilibrium. *J. Chem. Theory Comput.* **2012**, *8*, 348−362.

(11) Pérez, A.; Marchán, I.; Svozil, D.; Sponer, J.; Cheatham, T. E., III; Laughton, C. A.; Orozco, M. Refinement of the AMBER Force Field for Nucleic Acids: Improving the Description of alpha/gamma Conformers. *Biophys. J.* **2007**, *92*, 3817−3829.

(12) Zinchenko, A. A.; Yoshikawa, K. Na+ Shows a Markedly Higher Potential than K+ in DNA Compaction in a Crowded Environment. *Biophys. J.* **2005**, *88*, 4118−4123.

(13) Bai, Y.; Greenfeld, M.; Travers, K. J.; Chu, V. B.; Lipfert, J.; Doniach, S.; Herschlag, D. Quantitative and Comprehensive Decomposition of the Ion Atmosphere Around Nucleic Acids. *J. Am. Chem. Soc.* **2007**, *129*, 14981−14988.

(14) Tolokh, I. S.; Pabit, S. A.; Katz, A. M.; Chen, Y.; Drozdetski, A.; Baker, N.; Pollack, L.; Onufriev, A. V. Why Double-Stranded RNA Resists Condensation. *Nucleic Acids Res.* **2014**, *42*, 10823−10831.

(15) Drew, H. R.; Wing, R. M.; Takano, T.; Broka, C.; Tanaka, S.; Itakura, K.; Dickerson, R. S. Structure of a B-DNA dodecamer: Conformation and Dynamics. *Proc. Natl. Acad. Sci. U.S.A.* **1981**, *78*, 2179−2183.

(16) Eichman, B. F.; Vargason, J. M.; Mooers, B. H. M.; Ho, P. S. The Holliday Junction in an Inverted Repeat DNA Sequence: Sequence Effects on the Structure of Four-Way Junctions. *Proc. Natl. Acad. Sci. U.S.A.* **2000**, *97*, 3971−3976.

(17) Julien, O.; Beadle, J. R.; Magee, W. C.; Chatterjee, S.; Hostetler, K. Y.; Evans, D. H.; Sykes, B. D. Solution Structure of a DNA Duplex Containing the Potent Anti-Poxvirus Agent Cidofovir. *J. Am. Chem. Soc.* **2011**, *133*, 2264−2274.

(18) Lemkul, J. A.; Savelyev, A.; MacKerell, A. D., Jr. Induced Polarization Influences the Fundamental Forces in DNA Base Flipping. *J. Phys. Chem. Lett.* **2014**, *5*, 2077−2083.

DOI: 10.1021/jz5024543
J. Phys. Chem. Lett. 2015, 6, 212−216

SUPPORTING INFORMATION

for

Differential Impact of the Monovalent Ions Li^+, Na^+, K^+ and Rb^+ on DNA Conformational Properties

Alexey Savelyev and Alexander D. MacKerell Jr.*

Department of Pharmaceutical Sciences, School of Pharmacy, University of Maryland, Baltimore, MD 21201

* Corresponding author

Mailing Address: 20 Penn Street, Room 629, Baltimore, MD 21201

Email: alex@outerbanks.umaryland.edu

Phone: (410) 706-7442

Fax: (410) 706-5017

1. MD Simulation Protocols

1.1 CHARMM Drude Polarizable and Additive C36 MD Simulations

Setup and MD simulations of all DNA systems, EcoRI, 1DCV and 2L8Q, were carried out using the CHARMM[1] (v. 36) and NAMD[2] (v. 2.9) programs. Each system was independently simulated in four aqueous buffers: LiCl, NaCl, KCl and RbCl at ~100 mM. In addition, EcoRI and 1DCV systems were simulated in a combined NaCl/Tris·HCl aqueous buffer using the additive C36 force field, as elaborated below.

Initial configurations were generated using the *additive* C36 forces field. Each duplex in the canonical B form conformation was solvated in a cubic box of size *l*~60 Å with the additive TIP3P[3] water models, neutralizing ions (Li^+, Na^+, K^+ or Rb^+) and an extra ~100 mM of the corresponding chloride salt (LiCl, NaCl, KCl or RbCl) and then simulated for several nanoseconds, as described elsewhere.[4] Briefly, NPT ensembles at 298 K and 1 atm were simulated with periodic boundary conditions, with the particle mesh Ewald (PME) method[5] used to treat electrostatic interactions, and with the SETTLE algorithm[6] used to constrain covalent bonds involving hydrogen atoms enabling the use of the 2 fs time step. The last snapshots from these short additive runs were taken as inputs for subsequent Drude polarizable MD simulations, while production runs of all additive simulations were continued for another 150 ns. NAMD[2] was used for MD simulations and the CHARMM-GUI[7] was utilized for the additive system setup.

All polarizable systems were solvated with the SWM4-NDP[8] water model; the number of water molecules as well as ions was identical to those in the additive systems. Polarizable systems were generated using the CHARMM utility 'GENERATE DRUDE' that automatically adds the Drude particles and lone pairs to the polarizable (non-hydrogen) atoms. A subsequent self-consistent relaxation of the Drude positions in the electric filed was carried out using a combination of the steepest descent and ABNR minimization algorithms while all non-hydrogen atoms were restrained (K=10000 kcal/mol·$Å^2$). For each system a short equilibration of the solvent and mobile ions was then performed by running a 500 ps MD simulation with all solute atoms (but not the Drude particles) restrained (K=1000 kcal/mol·$Å^2$), followed by an additional 1 ns equilibration of the entire system without any restraints, after which the production MD simulations were initiated. All equilibration runs were conducted with the CHARMM program, utilizing the Velocity-Verlet integrator (VV2)[9] in conjunction with the TPCONTROL (Temperature-Pressure Control) command, allowing for efficient simulation of the motion of Drude oscillators. In particular, a Nose-Hoover thermostat was applied to all real atoms to control the global system temperature at 300K, and a separate low-temperature thermostat at 1K was applied to Drude particles to ensure that their time course approximates the self-consistent field (SCF) regimen.[9] A constant pressure (1 atm) was maintained via a modified Andersen-Hoover barostat, and SHAKE[10] was used to constrain covalent bonds involving hydrogens. Electrostatic interactions were treated using PME[5] summation with a coupling parameter of 0.34 and a sixth-order spline for mesh interpolation. Non-bonded pair lists were maintained out to 16 Å, and a real space cutoff of 12 Å was used for the electrostatic and Lennard-Jones (LJ) terms, with a long-range correction applied to LJ interactions.[11] A recently implemented 'HARDWALL' feature of the CHARMM program enabled use of a 1 fs time step in MD simulations.[12] As previously described, this feature is associated with a "hard wall" reflective term in the potential energy function that has been added to resolve the possibility of polarization catastrophe in Drude MD simulations. This term was invoked only when Drude particles moved

>0.2 Å away from their parent nuclei during MD simulations. An analogous simulation protocol was used in all production MD runs with NAMD where an alternate dual thermostating approach is applied based on Langevin dynamics.[13] The SETLLE algorithm[6] was used to constrain covalent bonds involving hydrogens. The duration of all production runs was identical to those of the additive systems, 150 ns.

To closer match experimental conditions, two additional additive C36 runs, of 150 ns each, were carried out for 1DCV and EcoRI systems immersed in a combined ~100 mM NaCl and ~50 mM Tris·HCl ionic buffer. Tris·H (protonated '*tris(hydroxymethyl)aminomethane)*', chemical formula is $(HOCH_2)_3C–NH_3^+$) parameters were obtained from CGenFF.[14] Otherwise, the simulation conditions were identical to those used for the above-described additive systems with no Tris·HCl.

To understand if the duration of the MD simulations is satisfactory, we estimated the average residence time of the ions inside the minor groove and insured that it is much smaller than the time of entire simulation. This is important to verify as ions clearly modulate DNA conformation via penetrating the DNA minor groove, whose width strongly correlates with the type of the ion in the Drude polarizable simulations. A common practice is to require the MD simulation time be 2-3 orders of magnitude longer than the correlation time (average residence time of the ion inside the minor groove in our case) of the phenomena being studied. The ionic residence time was ~20-30 ps, about a factor of ~5000 shorter than the MD simulation times of 150 ns.

1.2 AMBER MD Simulations

MD simulations utilizing AMBER Parmbsc0 force field for nucleic acids,[15] Cheatham and Joung ionic parameters[16] and the TIP3P water model[3] were performed on 1DCV and EcoRI systems in NaCl aqueous buffer only. Periodic boundary conditions were used, with the sizes of simulation boxes identical to those of the additive C36 and Drude polarizable systems (l~60 Å). We built ideal B form DNA chain models using the AMBER14 suite of programs.[17-18] The initial positions of the Na^+ and Cl^+ ions were determined from the computed electrostatic potential using LEaP.[17] For system equilibration and production runs NAMD 2.9 was used.[2] We followed a multistage equilibration process, reported by Orozco and co-workers,[19] to equilibrate all starting structures. The subsequent production runs for both systems (150 ns) were carried out at constant temperature (300 K) and pressure (1 atm), using the Langevin temperature equilibration scheme and the Langevin piston Nose-Hoover method to control the pressure.[2] The PME method[5] was used to treat long-range interactions with a 12 Å non-bonded cutoff. The SETTLE algorithm[6] was used to constrain all bonds involving hydrogen atoms, enabling the use of the 2 fs time step without any instability.

2. Computation of the DNA Solution Scattering Profiles

We followed the methodology elaborated in Refs.[20-25] and implemented the subroutine for calculating DNA scattering profiles from MD trajectories using the Biochemical Algorithms Library (BALL).[26] The scattering intensity, an experimentally accessible value, is calculated as the product of the scattering amplitude of all atoms with its complex conjugate:

$$I(\mathbf{q}) = A \cdot A^* = \sum_i \sum_j b_i b_j \mathrm{e}^{i\mathbf{q}\mathbf{r}_{ij}},$$

where b_i, b_j are the atomic scattering amplitudes for the atoms i and j, respectively, $\mathbf{r}_{ij}$ is the radius-vector connecting these atoms, and $\mathbf{q}$ is the scattering vector. In solution the scattering intensity from the entire sample is isotropic and proportional to the scattering from a single particle averaged over all orientations Ω, resulting in the following expression,

$$I(q) = \langle I(\mathbf{q}) \rangle_\Omega = \sum_i \sum_j b_i b_j \frac{\sin qr_{ij}}{qr_{ij}}.$$

The vectorial quantities are now reduced to their absolute values. We follow Refs.[25, 27] and represent atomic scattering amplitudes as follows,

$$b_i = f_i(q) - \rho_0 g_i(q),$$

where $f_i(q)$ is atom *i's* scattering form factor (functional forms approximating atomic form factors as well as their parametrization can be found in numerous sources, e.g., web-site of the National Institute of Standards and Technology, NIST[28]), ρ_0 is the electron density of the solvent, and $g_i(q)$ is the form factor of the dummy atoms located at the same positions $\mathbf{r}_i$ as real atoms and accounting for the excluded (for solvent) volume; this last term is expressed as

$$g_i(q) = G(q) V_i \mathrm{e}^{-q^2 V_i^{2/3}/4\pi},$$

where V_i is the solvent volume displaced by the atom i, or group of atoms, centered at r_i and represented by a Gaussian sphere of the appropriate radius (those values are available, e.g. at the NIST web-site[28]); $G(q)$ is an independent on atomic positions overall expansion factor,

$$G(q) = (V_0 / V_m) e^{-q^2 (V_0^{2/3} - V_m^{2/3})/4\pi},$$

with V_0 being an effective atomic volume, a variable parameter (see below), and V_m an average volume of the atomic group. As elaborated in Refs.[25, 27], the expansion factor accounts for solvent displacement by the solute and can be adjusted by changing the ratio of the dummy atom radius to the average atomic van der Waals radius, $R_{0m} = r_0/r_m$, to bring the calculated and experimental scattering amplitudes into better agreement. In other words, tuning of R_{0m} has the effects of changing the scattering contrast. In light of our DNA problem, it was suggested that adjustment of R_{0m} is likely to partially account for the presence of the cloud of counter-ions (ionic atmosphere) in the vicinity of DNA not considered in the calculated scattering spectra. Importantly, these adjustments were demonstrated to alter only the scattering background and not the spectral patterns.[25, 27]

Additional comment on the inherent differences between experimental and computational X-ray spectra is in order. Indeed, intensity scales are quite different with the major

peaks more diffuse in the experimental versus the simulation profiles. This is because experimental data are collected on a huge number DNA molecules over a long period of time, both of which impacts the intensity of the spectra as well as the broadness of the peaks. In contrast, in MD simulations with periodic boundary conditions only a single molecule is present (despite being at approximately the same concentration of DNA used in the experiment), which inherently disallows the intensity and peak shapes of the calculated spectra to match that from experiment. That is why the number of peaks and their positions are the most important characteristics to compare.

3. DNA Structural Analysis

RMS differences for all non-hydrogen atoms in the non-terminal nucleotides were calculated relative to the ideal B forms for 1DCV and EcoRI sequences. Drude, C36 and AMBER models were compared. CHARMM analysis tools[1] were used for these calculations. In addition, distributions for selected DNA helicoidal parameters (roll, twist, slide, groove width etc.) were computed using the Curves package.[29-30] Variations of those parameters with the change of the ion type used in an aqueous buffer were monitored. Preceding these calculations, MD trajectories were reimaged/recentered using our in-house routing written with BALL[26]; such post-processing was necessary for subsequent calculations of the overall DNA properties (RMSD, helicoidal parameters), since DNA strands (treated as independent segments) appeared separated in the course of simulation because of the periodic boundary conditions.

Table S1. Statistics on the minor groove width distributions shown in Fig. 3. Mean values (AVE), standard deviations (SD) and standard errors (SE) are provided. Standard errors are estimated as standard deviations of the mean values computed based on trajectory decomposition into 10 blocks of 15 ns each. Values are in Angstroms.

		1DCV				**EcoR1**				**2L8Q**			
		Li+	Na+	K+	Rb+	Li+	Na+	K+	Rb+	Li+	Na+	K+	Rb+
DRUDE	AVE	6.34	7.61	8.15	8.27	7.71	7.99	8.04	8.09	7.12	7.50	8.00	8.15
	SD	1.96	1.77	1.74	1.70	1.89	1.39	1.33	1.60	1.84	1.65	1.56	1.57
	SE	0.22	0.21	0.17	0.19	0.21	0.17	0.18	0.19	0.25	0.22	0.20	0.19
C36	AVE	7.91	7.85	7.99	7.91	7.47	7.41	7.34	7.29	8.43	8.20	7.96	8.20
	SD	1.54	1.47	1.49	1.51	1.46	1.45	1.62	1.72	1.32	1.32	1.31	1.42
	SE	0.10	0.11	0.11	0.11	0.12	0.10	0.11	0.11	0.13	0.11	0.12	0.10

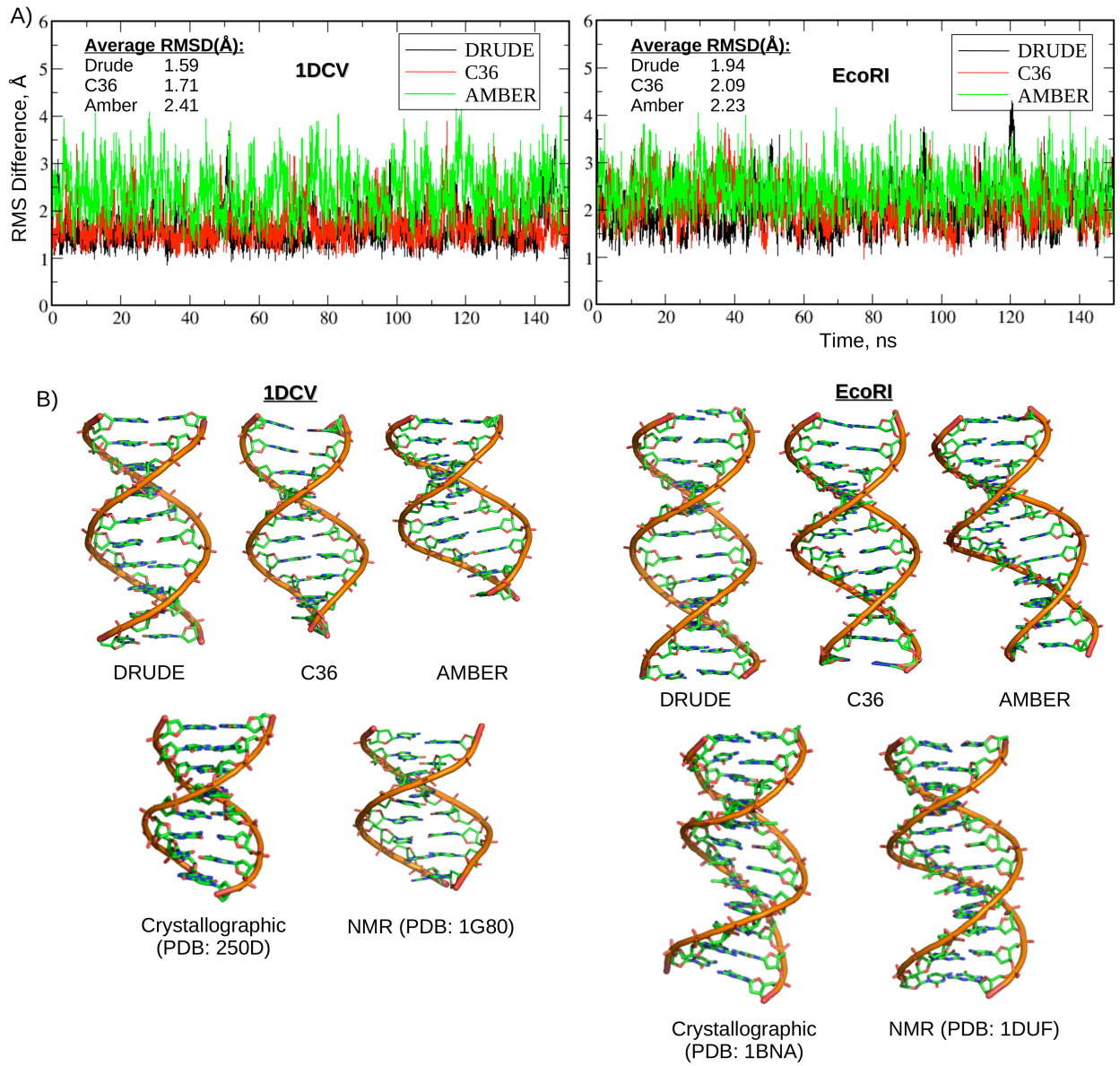

Figure S1. (A) RMS difference versus time for the 1DCV and EcoRI systems with respect to the canonical B forms computed from MD simulations utilizing Drude polarizable (black), CHARMM additive C36 (red) and the AMBER (additive) Parmbsc0 (green) force fields. Also listed are the RMSD values averaged over the entire trajectory. (B) 1DCV and EcoRI structures averaged over the entire trajectories. Also shown are selected crystallographic and NMR structures (for 1DCV only internal 8 base pairs are shown). Structures are aligned with respect to the upper half of the molecule against the Drude model for convenience.

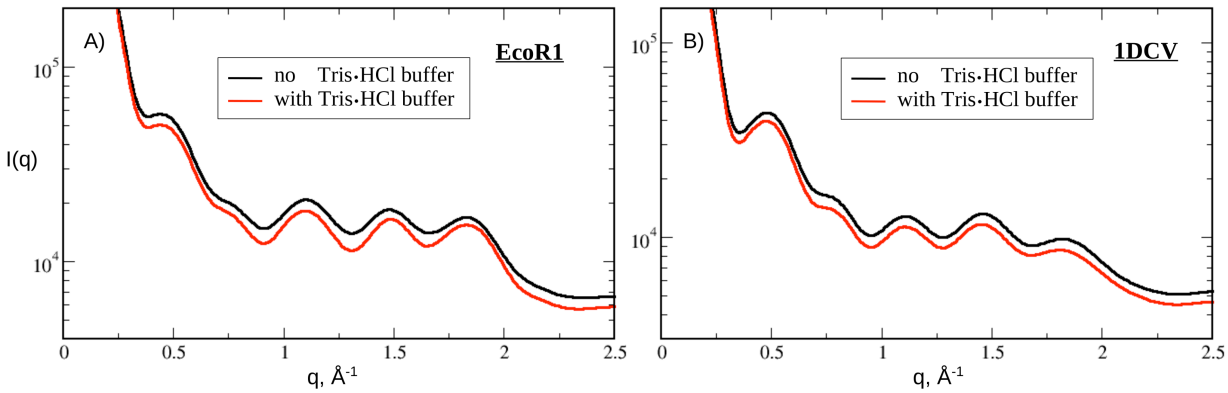

Figure S2. Solution scattering profiles for the EcoRI and 1DCV systems computed from the CHARMM additive (C36) MD simulations with and without addition of an extra ~50 mM Tris·HCl buffer to the ~100mM NaCl.

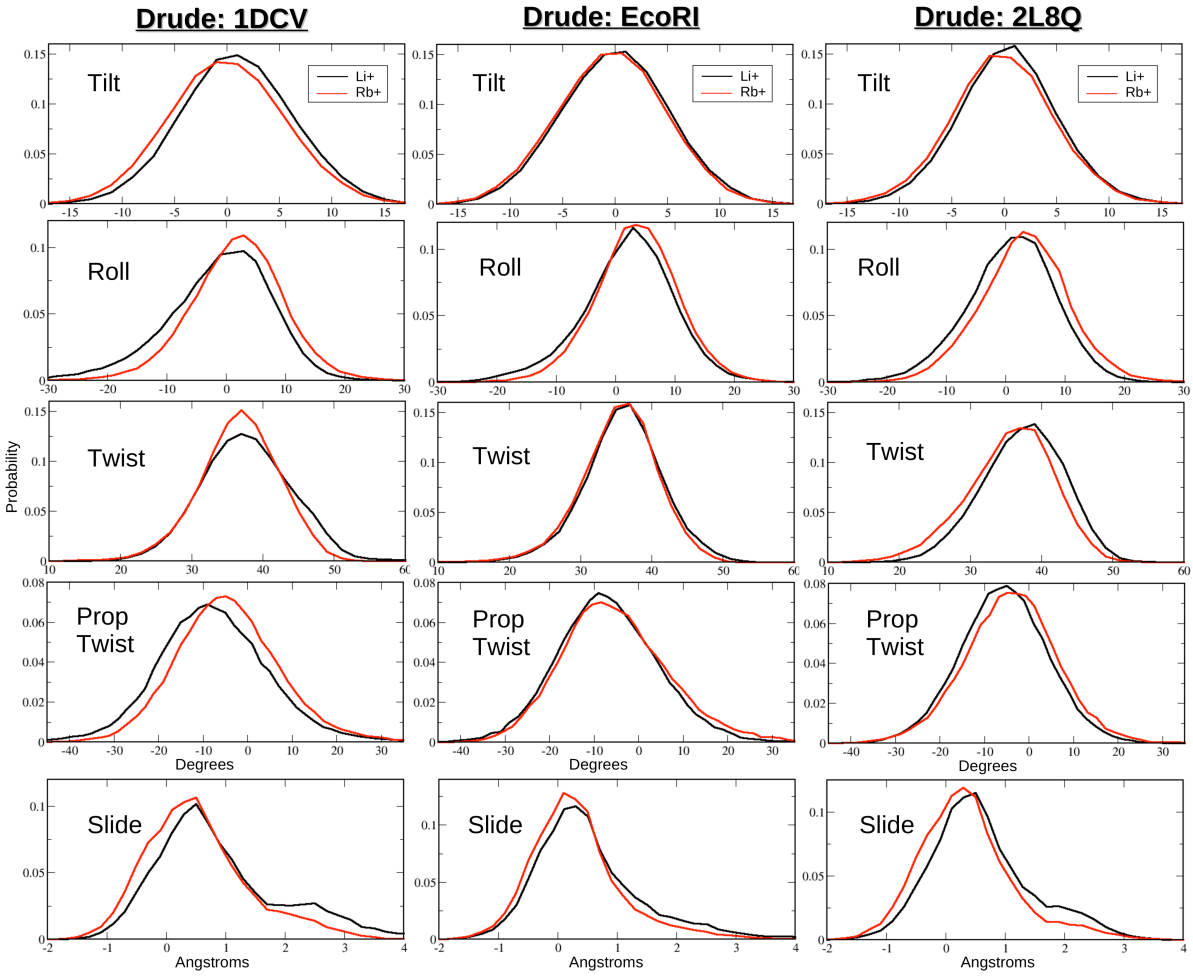

Figure S3. Probability distributions for selected helicoidal parameters computed from the Drude polarizable MD simulations of the 1DCV, EcorI and 2L8Q DNA systems solvated in the LiCl (black) and RbCl (red) aqueous buffers. Because these are the extreme cases generating the biggest variations in the spectral patterns we omit the results for NaCl and KCl for clarity.

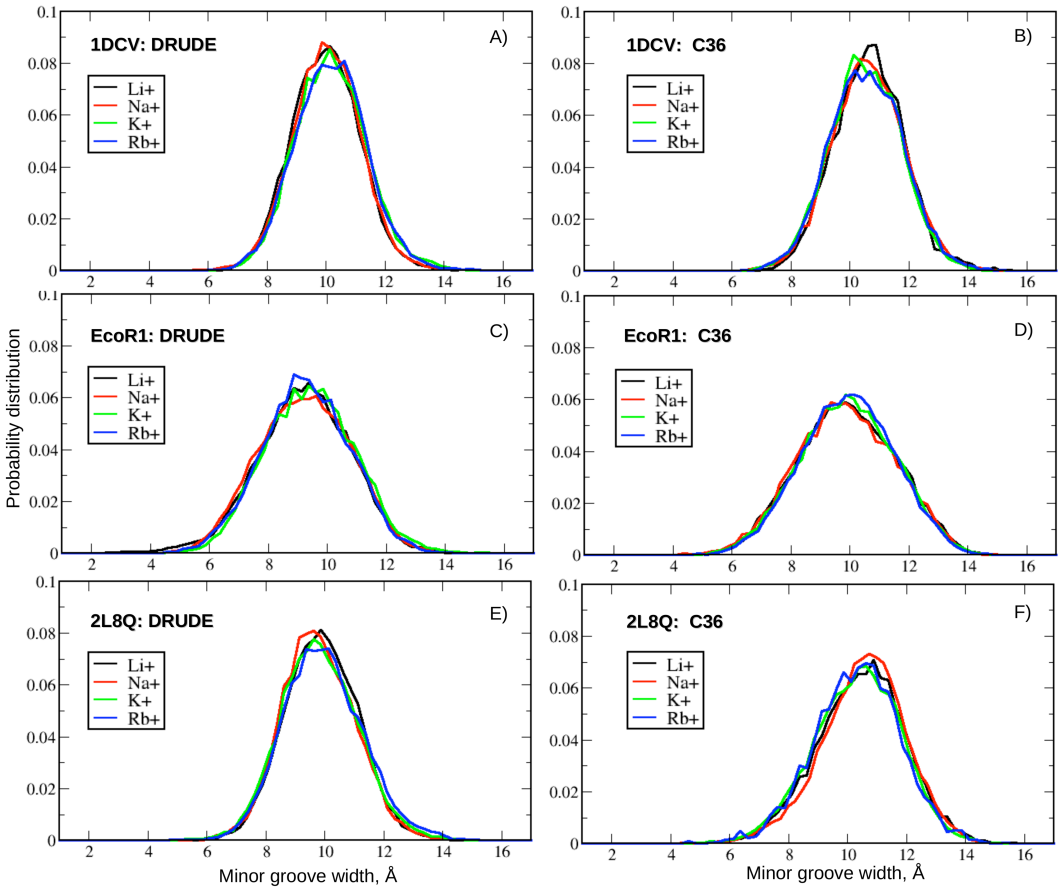

Figure S4. Probability distributions for the major groove width computed from the Drude polarizable and additive CHARMM36 MD simulations of the 1DCV, EcoRI and 2L8Q DNA systems solvated in various monovalent ionic buffers.

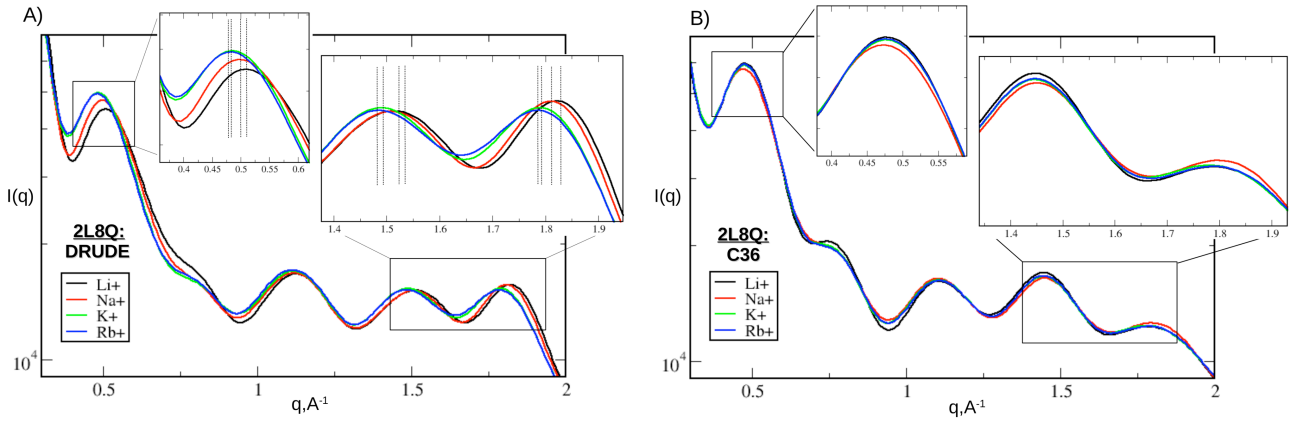

Figure S5. Solution scattering profiles computed from the Drude polarizable (A) and C36 additive (B) MD simulations of the 2L8Q DNA molecule solvated in LiCl, NaCl, KCl and RbCl ionic buffers. For the Drude model demonstrating spectral variability with the ion type the approximate positions of the first and two last peaks are shown.

REFERENCES

(1) Brooks, B. R.; Brooks III, C. L.; MacKerell Jr., A. D.; Nilsson, L.; Petrella, R. J.; Roux, B.; Won, Y.; Archontis, G.; Bartels, C.; Boresch, S.; Caflisch, A.; Caves, L.; Cui, Q.; Dinner, A. R.; Feig, M.; Fischer, S.; Gao, J.; Hodoscek, M.; Im, W.; Kuczera, K.; Lazaridis, T.; Ma, J.; Ovchinnikov, V.; Paci, E.; Pastor, R. W.; Post, C. B.; Pu, J. Z.; Schaefer, M.; Tidor, B.; Venable, R. V.; Woodcock, H. L.; Wu, X.; Yang, W.; York, D. M.; Karplus, M. CHARMM: The biomolecular simulation program. *J. Comput. Chem.* **2009,** *30*, 1545-1614.

(2) Phillips, J. C.; Braun, R.; Wang, W.; Gumbart, J.; Tajkhorshid, E.; Villa, E.; Chipot, C.; Skeel, R. D.; Kale, L.; Schulten, K. Scalable molecular dynamics with NAMD. *J. Comput. Chem.* **2005,** *26*, 1781-1802.

(3) Jorgensen, W. L.; Chandrasekhar, J.; Madura, J. D.; Impey, R. W.; Klein, M. L. Comparison of simple potential functions for simulating liquid water. *J. Chem. Phys.* **1983,** *79*, 926.

(4) Hart, K.; Foloppe, N.; Baker, C. M.; Denning, E. J.; Nilsson, L.; MacKerell, A. D., Jr. Optimization of the CHARMM Additive Force Field for DNA: Improved Treatment of the BI/BII Conformational Equilibrium. *J. Chem. Theory Comput.* **2012,** *8*, 348-362.

(5) Darden, T. A.; York, D.; Pedersen, L. G. Particle mesh Ewald: An Nlog(N) method for Ewald sums in large systems. *J. Chem. Phys.* **1993,** *98*, 10089-10092.

(6) Miyamoto, S.; Kollman, P. SETTLE: An Analytical Version of the SHAKE and RATTLE Algorithm for Rigid Water Models. *J. Comput. Chem.* **1992,** *13*, 952–962.

(7) Jo, S.; Kim, T.; Iyer, V. G.; Im, W. CHARMM-GUI: a web-based graphical user interface for CHARMM. *J. Comput. Chem.* **2008,** *29*, 1859-65.

(8) Lamoureux, G.; Harder, E.; Vorobyov, I. V.; Roux, B.; MacKerell, A. D., Jr. A polarizable model of water for molecular dynamics simulations of biomolecules. *Chem. Phys. Lett.* **2006,** *418*, 245-249.

(9) Lamoureux, G.; Roux, B. Modeling induced polarization with classical Drude oscillators: Theory and molecular dynamics simulation algorithm. *J. Chem. Phys.* **2003,** *119*, 3025-3039.

(10) Ryckaert, J. P.; Ciccotti, G.; Berendsen, H. J. C. Numerical Integration of the Cartesian Equations of Motion of a System with Constraints: Molecular Dynamics of n-alkanes. *J. Comput. Phys.* **1977,** *23*, 327-341.

(11) Allen, M. P.; Tildesley, D. J., *Computer simulation of liquids*. Oxford University Press: Oxford, 1987.

(12) Chowdhary, J.; Harder, E.; Lopes, P. E.; Huang, L.; MacKerell, A. D., Jr.; Roux, B. A Polarizable Force Field of Dipalmitoylphosphatidylcholine Based on the Classical Drude Model for Molecular Dynamics Simulations of Lipids. *J. Phys. Chem. B* **2013,** *117*, 9142–9160.

(13) Jiang, W.; Hardy, D. J.; Phillips, J. C.; Mackerell, A. D., Jr.; Schulten, K.; Roux, B. High-performance scalable molecular dynamics simulations of a polarizable force field based on classical Drude oscillators in NAMD. *J Phys Chem Lett* **2011,** *2*, 87-92.

(14) Vanommeslaeghe, K.; Hatcher, E.; Acharya, C.; Kundu, S.; Zhong, S.; Shim, J.; Darian, E.; Guvench, O.; Lopes, P.; Vorobyov, I.; Mackerell, A. D. CHARMM general force field: A force field for drug-like molecules compatible with the CHARMM all-atom additive biological force fields. *J. Comput. Chem.* **2010,** *31*, 671-690.

(15) Perez, A.; Marchan, I.; Svozil, D.; Sponer, J.; Cheatham, T. E.; Laughton, C. A.;

Orozco, M. Refinenement of the AMBER force field for nucleic acids: Improving the description of alpha/gamma conformers. *Biophys. J.* **2007,** *92*, 3817-3829.

(16) Joung, I. S.; Cheatham, T. E. Determination of alkali and halide monovalent ion parameters for use in explicitly solvated biomolecular simulations. *J. Phys. Chem. B* **2008,** *112*, 9020-9041.

(17) Case, D. A.; Cheatham, T. E.; Darden, T.; Gohlke, H.; Luo, R.; Merz, K. M.; Onufriev, A.; Simmerling, C.; Wang, B.; Woods, R. J. The Amber biomolecular simulation programs. *J. Comput. Chem.* **2005,** *26*, 1668-1688.

(18) D.A. Case; V. Babin; J.T. Berryman; R.M. Betz; Q. Cai; D.S. Cerutti; T.E. Cheatham, I.; T.A. Darden; R.E. Duke; H. Gohlke; A.W. Goetz; S. Gusarov; N. Homeyer; P. Janowski; J. Kaus; I. Kolossvary; A. Kovalenko; T.S. Lee; S. LeGrand; T. Luchko; R. Luo; B. Madej; K.M. Merz; F. Paesani; D.R. Roe; A. Roitberg; C. Sagui; R. Salomon-Ferrer; G. Seabra; C.L. Simmerling; W. Smith; J. Swails; R.C. Walker; J. Wang; R.M. Wolf; X. Wu; Kollman, P. A. AMBER 14. *University of California, San Francisco* **2014**.

(19) Shields, G. C.; Laughton, C. A.; Orozco, M. *J. Am. Chem. Soc.* **1998,** *120*, 5895-5904.

(20) Svergun, D.; Barberato, C.; Koch, M. H. J. CRYSOL - A program to evaluate x-ray solution scattering of biological macromolecules from atomic coordinates. *J. Appl. Crystallogr.* **1995,** *28*, 768-773.

(21) Zhang, R. T.; Thiyagarajan, P.; Tiede, D. M. Probing protein fine structures by wide angle solution X-ray scattering. *J. Appl. Crystallogr.* **2000,** *33*, 565-568.

(22) Tiede, D. M.; Zhang, R. T.; Seifert, S. Protein conformations explored by difference high-angle solution x-ray scattering: Oxidation state and temperature dependent changes in cytochrome C. *Biochemistry* **2002,** *41*, 6605-6614.

(23) Tiede, D. M.; Zhang, R. T.; Chen, L. X.; Yu, L. H.; Lindsey, J. S. Structural characterization of modular supramolecular architectures in solution. *J. Am. Chem. Soc.* **2004,** *126*, 14054-14062.

(24) Zuo, X.; Tiede, D. M. Resolving Conflicting Crystallographic and NMR Models for Solution-State DNA with Solution X-ray Diffraction. *J. Am. Chem. Soc.* **2005,** *127*, 16-7.

(25) Zuo, X. B.; Cui, G. L.; Merz, K. M.; Zhang, L. G.; Lewis, F. D.; Tiede, D. M. X-ray Diffraction "Fingerprinting" of DNA Structure in Solution for Quantitative Evaluation of Molecular Dynamics Simulation. *Proc. Nat. Acad. Sci. USA* **2006,** *103*, 3534-3539.

(26) Kohlbacher, O.; Lenhof, H. P. BALL - rapid software prototyping in computational molecular biology. *Bioinformatics* **2000,** *16*, 815-824.

(27) Zuo, X. B.; Tiede, D. M. Resolving Conflicting Crystallographic and NMR Models for Solution-State DNA with Solution X-ray Diffraction. *J. Am. Chem. Soc.* **2005,** *127*, 16-7.

(28) www.nist.gov/pml/data/ffast/.

(29) Lavery, R.; Sklenar, H. The definition of generalized helicoidal parameters and of the axis of curvature for irregular nucleic acids. *J. Biomol. Str. Dyn.* **1988,** *6*, 63-91.

(30) Ravishanker, G.; Swaminathan, S.; Beveridge, D. L.; Lavery, R.; Sklenar, H. Conformational and Helicoidal Analysis of 30 ps of Molecular Dynamics on the d(CGCGAATTCGCG) Double Helix: "Curves", Dials and Windows. *J. Biomol. Str. Dyn.* **1989,** *6*, 669-699.